Peculiarities of Gas Ejection Into Vacuum From a Nozzle With Near-Wall Liquid Film

V.G. Prikhodko, S.F. Chekmarev, I.V. Yarygin, V.N. Yarygin

Kutateladze Institute of Thermophysics SB RAS, Novosibirsk, Russia
yarygin@itp.nsc.ru

Abstract. Ejection of gas into vacuum from a nozzle with near-wall liquid film is being studied in this paper. Experimental investigation of the flow shows that a near-wall liquid film flowing down on an inner surface of the nozzle not only breaks up into droplets at the output edge of the nozzle but also emerges onto the external surface of the nozzle, moving backwards on it, even opposite to gravity.

Keywords: Vacuum, nozzle, near-wall liquid film, droplets, backflow.
PACS: 47.40.Ki, 47.45.-n, 47.60.+i, 47.61.Jd

INTRODUCTION

This study was initiated by the problem of external contamination of the surfaces of space vehicles (including the International Space Station) by jets of orientation and control engines, where a fuel film is used for cooling nozzle walls [1]. Although gas jet expansion into vacuum has been studied in numerous experimental and theoretical works, the problem of joint gas flow with a near-wall liquid film has not yet been systematically investigated. At ejection into vacuum liquid becomes instantly overheated owing to strong pressure decreasing that leads to its explosive disintegration on drops. A gas-droplet flow including two substantially different regions of the droplet-phase flow – central and peripheral – is then formed behind the nozzle edge [1]. The central region is characterized by the presence of high-velocity (approximately hundreds of meters per second) small (about micron) droplets and is formed due to the stripping of droplets from the film surface by an aircraft gas flow in the near-critical section of the nozzle, to their further breakdown and acceleration in the flow inside the nozzle and in the jet behind it. The angular size of this region with respect to the jet axis reaches 30°. The peripheral region of the droplet-phase flow is characterized by the presence of low-velocity (about a meter per second), relatively large (approximately hundreds of microns) droplets and is formed due to the dispersion of the near-wall liquid film on the outlet nozzle edge. This region can cover from 30° to 180° with respect to the nozzle axis, and back (at angles > 90° with respect to the nozzle axis) flows of the droplet phase are formed in this region. Although both regions of the droplet-phase flow are of interest, the investigation of the peripheral region is more urgent, because reverse flows that are responsible for external pollution of the surfaces of space vehicles and space stations are formed in this region [1].

EXPERIMENTAL SETUP AND MEASUREMENT TECHNIQUES

Experiments were carried out on a VIKING vacuum gas-dynamic setup of the Kutateladze Institute of Thermophysics [2]. The large volume of the working chamber (150 m^3) provided operation in the pulse mode with high flow rates of a gas and liquid. The injected liquid was completely evaporated and evacuated by normal vacuum pumps.

The gas and liquid were fed from a gas-dynamic source, which made it possible to vary their flow rates and to change output sections of the nozzles. As such nozzles, we used a cylindrical tube 5 mm in diameter and a conic supersonic nozzle, which had a semiangle of $\alpha = 7°$; radii of critical and output sections of 5 and 10 mm, respectively; and a cylindrical external surface. In both cases, the thickness of the output section edge was equal to $l = 1$ mm. The nozzles were arranged vertically with the output section facing downwards.

The liquid entered through a circular gap in the premix chamber of the nozzle and flew down the nozzle walls as a film. Simultaneously, a gas was blown through the nozzle. At the nozzle exit, a supersonic freely expanding jet of vapor-gas mixture with dispersed liquid droplets was formed. We used air as the working gas and ethanol as the working liquid. The structure of the formed flow depended on the parameters of gas and liquid in the premix chamber and pressure p_∞ in the vacuum chamber. The flow was recorded by video and photography. In addition a laser-knife method was used. The structure of the droplet-phase flow was visualized by means of a 30-mW semiconductor laser, which can operate both in the continuous and pulsed modes. The latter mode was used for stroboscopic illumination with a burst frequency of 10 Hz to 5 kHz and a burst duration of 1 to 255 μs. Images of the general structure of the flow were obtained and the size and velocity distribution functions were measured for droplets flowing into vacuum.

RESULTS OF EXPERIMENTS AND THEIR ANALYSIS

Photographs of the cylindrical nozzle (Fig. 1) show how the structure of the flow changes with a decrease in pressure in the vacuum chamber. Figures 1a and 1b refer to the flows into space with low ($p_\infty \approx 10$ Pa) and atmospheric pressure, respectively. It is seen that the flow into vacuum is accompanied by the appearance of a 1-mm-thick liquid film on the outer surface of the nozzle. The same pattern is also observed in the case of the supersonic nozzle.

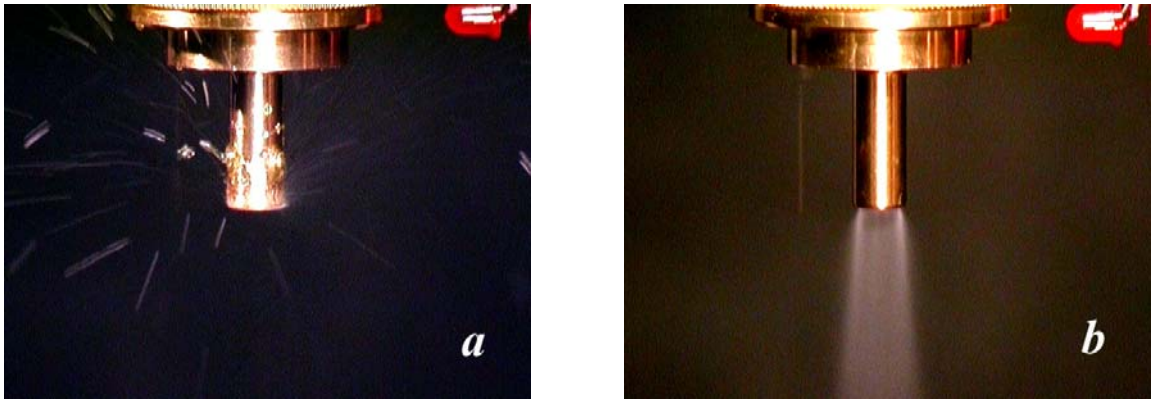

FIGURE 1. Influence of ambient pressure on the flow structure. *a* – flow into vacuum, *b* – flow into atmosphere

Figures 2a and 2b show the film rise height measured at various pressures in the vacuum chamber for the tube and supersonic nozzle, respectively. The stagnation pressure p_0 was equal to about $1.3 \cdot 10^5$ and 10^5 Pa in the first and second cases, respectively. The stagnation temperature was equal to 300 K in both cases. The mass flow rate of the liquid was equal to about 10% of that of the gas. Figures 4-5 show results of measurements of the size and velocity distribution functions for the nozzle in the form of a cylindrical tube 5 mm in diameter.

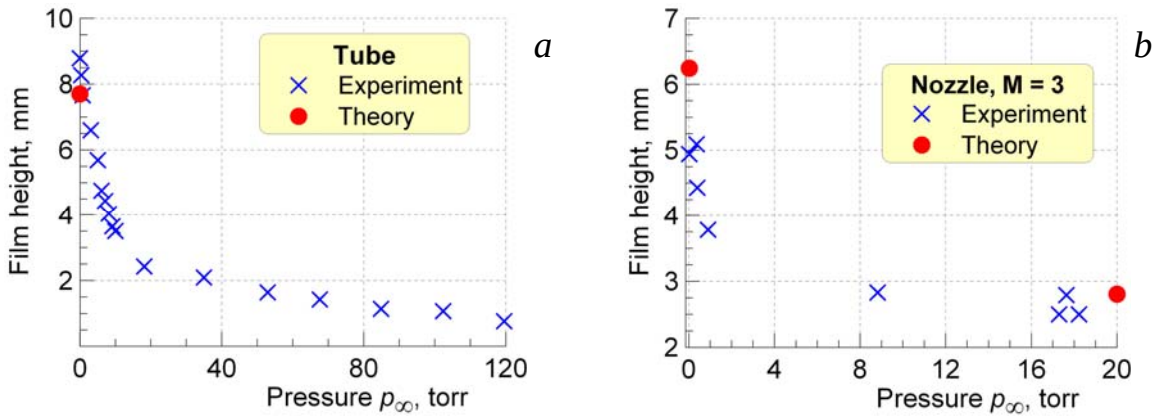

FIGURE 2. Film height on external surface. *a* – tube, *b* – supersonic nozzle

The analysis of experimental results leads to the following scheme of the stationary regime of flow formation. When the gas and liquid are injected, a liquid film is formed on the internal wall of the nozzle; under the influence of the gas stream and gravity, mainly owing to the first factor, the film moves to the nozzle edge. At the nozzle edge, the film turns and goes out onto the external surface of the nozzle. Film turning is stipulated by forces of adhesion and, probably, the Coanda effect, and film lifting is caused by interaction with the gas stream. Thus, there exists a maximum height h_m of film lifting, which depends on the gas-stream and liquid parameters. Accordingly, there is a certain, critical amount of liquid that can be contained in the film. Therefore, as soon as this amount of liquid in the film is accumulated, the stationary condition of the flow is formed: there is a film of height h_m on the external surface of the nozzle, and all new incoming liquid is carried away by the jet from the lower edge of the nozzle in the form of drops. Disintegration of the film into drops occurs owing to the Rayleigh-Taylor instability of the film under the influence of both the gas stream and gravity.

Under conditions of the experiments (the nozzle is mounted vertically with the exit cross section directed downward), the height of film lifting h_m can be estimated from the balance of forces on the film [3]

$$\rho_l g h_m = p_{g1} - p_{g2} + p_L \tag{1}$$

where ρ_l is the density of the liquid, g is the acceleration of gravity, p_{g1} and p_{g2} are the pressures in the gas at the bottom and top edges of the film, and p_L is the Laplace pressure at the bottom edge of the film, which in this case equals σ/r, where σ is the surface tension of the liquid and r is the radius of curvature of the film. For ethanol, ρ_l = 0.79 g/cm^3 and σ = 0.022 N/m.

Taking into account that the characteristic thickness of the film inside the nozzle (≈ 0.1 mm) is much smaller than the edge thickness l, and the thickness of the film on the external surface is commensurable with l, it can be assumed that $r = l$ for calculation of the Laplace pressure; in both cases (for cylindrical and conical nozzles), we have p_L = 22 Pa.

It is possible to use the pressure reached at turning by 90° in the Prandt-Mayer wave of the gas flow with a Mach number at the nozzle-exit cross section $\mathrm{M}_C = 1$ and a ratio of specific heats γ = 1.4 as p_{g1} for a cylindrical nozzle. Then, $p_{g1}/p_0 \approx 2.9 \cdot 10^{-4}$, and we obtain $p_{g1} \approx 39$ Pa for conditions of the experiments in Fig. 2a. The same value of p_{g1}/p_0 can also be accepted for a conical nozzle, taking into account that there is a boundary layer inside the nozzle; therefore, close to the nozzle edge, the value M = 1 is more typical rather than the "geometrical" value M_C = 3. In this case, we have $p_{g1} \approx 29$ Pa.

As to pressure on the top border of the film, it depends on a number of factors (jet pressure ratio, its rarefaction, etc.) and generally requires numerical calculation of the flow field. However, there are two cases, when the estimations can be carried out without numerical modeling. In the first case, the expansion occurs practically into vacuum ($p_\infty \approx 0$), and the value of p_{g2} can be neglected. As a result, using expression (2.5), we obtain $h_m \approx 7.7$ mm for a cylindrical nozzle and $h_m \approx 6.6$ mm for a conical nozzle. The second case corresponds to conditions of an isobaric jet $p_C = p_\infty$, which occurs in experiments with a conical nozzle. Here, $p_{g1} = p_{g2}$, and formula (1) predicts $h_m \approx 2.8$ mm. As is visible in Figs. 2a and 2b, which show the values of h_m by filled circles, the theoretical estimations correspond to the experimental data fairly well. It gives grounds to hope that the simple model proposed takes into account the major factors determining film formation on the external surface the nozzle.

According to this scheme, the time variation of the droplet-size distribution at the nozzle edge can be described by the kinetic equation

$$\frac{\partial n_g}{\partial t} = \beta_{g-1} n_{g-1} - \beta_g n_g - \gamma_g n_g , \tag{2}$$

where n_g is the number of droplets containing g molecules; β_g and γ_g are the rates of the droplet growth and shedding, respectively. Measuring the drop size by the drop volume $v = g v_1$, where v_1 is the liquid volume per one molecule, and assuming the drops to be large enough, so that $\beta_{g-1} n_{g-1} \approx \beta_g n_g - \partial(\beta_g n_g)/\partial g$, we can rewrite Eq. (2) as

$$\frac{\partial n_\nu}{\partial t} + \frac{\partial(\beta_\nu n_\nu)}{\partial \nu} = -\gamma_\nu n_\nu .$$

The steady solution of this equation is

$$n_\nu = \frac{C}{\beta_\nu} \exp\left(-\int_0^\nu \omega_\nu \, d\nu \right),$$

where

$$\omega_\nu = \gamma_\nu / \beta_\nu \tag{3}$$

and C is the normalizing factor. Correspondingly, the distribution function of the shed droplets is written as

$$p_\nu = \gamma_\nu n_\nu = C\omega_\nu \exp\left(-\int_0^\nu \omega_\nu \, d\nu \right). \tag{4}$$

Assume that the growth of droplets is determined by liquid inflow from the film, with the rate of the influx into the ν-th droplet being proportional to the droplet cross-section S_ν. Then the droplet growth rate β_ν is

$$\beta_\nu = \frac{S_\nu G_l}{\rho_l A}, \tag{5}$$

where G_l is the total discharge of the liquid, ρ_l is the liquid density, and A is a constant, having the meaning of the total cross-section of the droplets $S_{\text{tot}} = \int S_\nu n_\nu \, d\nu$.

To estimate the rate of droplet shedding, γ_g, we used the following model. Let the droplet of ν-th size be shed, under the gas flow forcing, with the probability

$$P_{\text{tear}} = \exp\left(-\alpha / We_\nu\right), \tag{6}$$

where

$$\text{We}_\nu = 2\rho_g {u_g}^2 r_\nu \big/ \sigma \tag{7}$$

is the Weber number, ρ_g and u_g are the density and velocity of the gas flow, r_ν is the drop radius, and σ is the surface tension of the liquid. After shedding, the droplet is transported by the gas flow turning around the nozzle edge, which affects the droplet with a force equal to $\rho_g {u_g}^2 S_\nu$. Thus, the droplet performs a uniformly accelerated motion, with the acceleration equal to

$$a_\nu = \frac{\rho_g {u_g}^2 S_\nu}{\rho_l \nu}, \tag{8}$$

and passes a distance equal to its diameter, $2r_\nu$, i.e. is shed from the liquid film, during the time

$$t_\nu = \left(\frac{4 r_\nu \rho_l \nu}{\rho_g {u_g}^2 S_\nu} \right)^{1/2}. \tag{9}$$

Correspondingly, the droplet shedding rate $\gamma_\nu = P_{\text{tear}}(\text{We}) \big/ t_\nu$ is expressed as

$$\gamma_\nu = \left(\frac{\rho_g {u_g}^2 S_\nu}{4 r_\nu \rho_l \nu} \right)^{1/2} \exp\left(-\frac{\alpha}{\text{We}_\nu} \right). \tag{10}$$

Substituting Eqs. (5) and (10) into Eqs. (3)-(4) and performing integration in Eq. (4), we obtain for the droplet distribution on radius $p_r = 4\pi r^2 p_\nu$

$$p_r = C \frac{K}{r} \exp\left\{ -\left[K E_1\left(\frac{\alpha}{\text{We}_r} \right) + \frac{\alpha}{\text{We}_r} \right] \right\}. \tag{11}$$

Here

$$K = \frac{\left(3\rho_g u_g{}^2 \rho_l\right)^{1/2} A}{G_l} \tag{12}$$

is a dimensionless complex of parameters, $E_1(x) = \int_1^\infty \exp(-xt)\,dt/t$ is the integral exponential function, We_r is the local Weber number (7), and C is a constant defined by the condition $\int_0^\infty p_r dr = 1$.

The distribution function given by Eq. (11) is shown in Fig. 3 by the solid curve. Here, according to the test conditions, ρ_l = 0.8 g/cm^2, σ = 0.022 N/m, T_0 = 300 K, p_0 = 1.2·10^5 Pa, and G_l = 0.5 g/s. The values of ρ_g and u_g were the gas density and velocity obtained in the Prandtl-Meyer flow turning at an angle of 90° around the nozzle lip, which gave ρ_g = 3.4·10^{-6} g/cm^3 and u_g = 7·10^2 m/s (M_g = 6.85). The constants A and α, entering Eqs. (5) and (6), were fitted to reach the best agreement of the theoretical distribution (11) with the experimental data, and were obtained as A = 5.7·10^{-3} and α = 25. It is seen that the theoretical relation (11) reproduces the size distribution of droplets quite well. In particular, Eq. (11), which is independent of the nozzle-lip shape, agrees with the experimental data in terms of the weak effect of the nozzle-lip shape on the behavior of droplets. Note also that the value of $S_{\mathrm{tot}} = \int S_\nu\, n_\nu\, d\nu$ calculated with the help of Eq. (11) shows that the effective cross-section of the droplet for the liquid influx into the droplet is approximately equal to $0.67 \cdot S_\nu$.

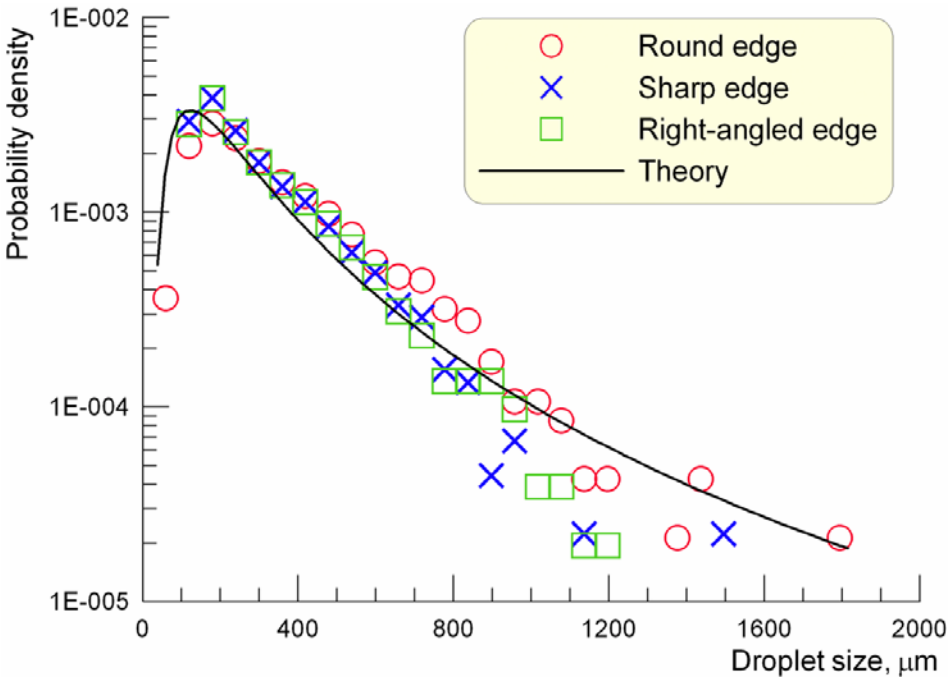

FIGURE 3. Distribution of droplets on sizes. Tube of 5 mm diameter.

This model can, in principle, be extended to describe the direction-of-flight and velocity distribution functions of droplets, which requires a consideration of droplet interaction with a gas flow expanding behind the nozzle exit. In this connection, note that, according to the model, the velocity of the droplet after its shedding from the liquid film is

$$V_\nu = a_\nu\, t_\nu = \left(4\rho_g u_g{}^2 r_\nu S_\nu / \rho_l \nu\right)^{1/2},$$

where a_v and t_v are defined by Eqs. (8) and (9), respectively. For the conditions of the present experiments, this equation yields V_v = 2.5 m/s, which is in good agreement with the experimental data by the order of magnitude (see Fig. 4).

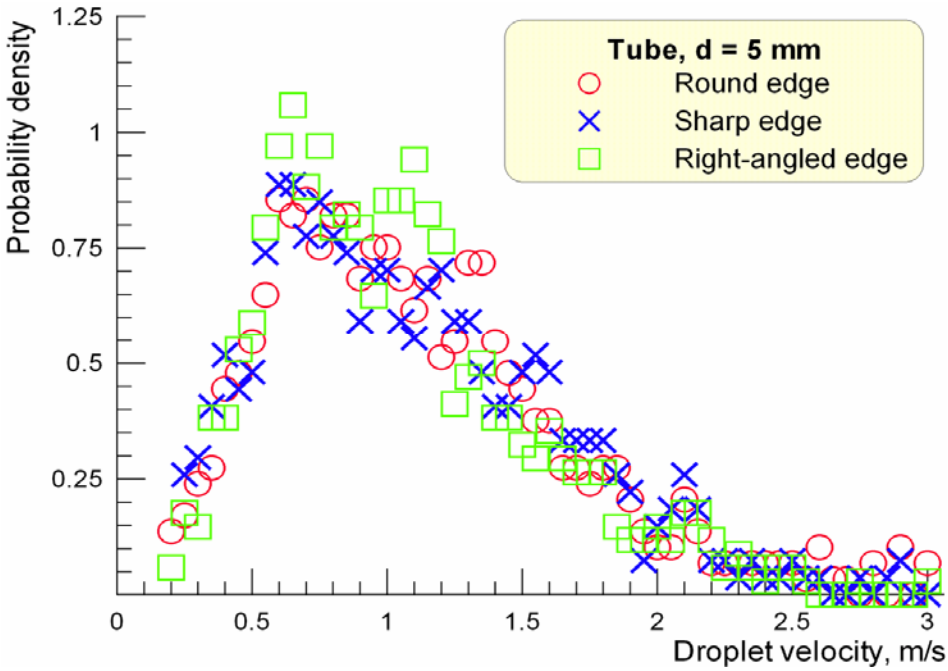

FIGURE 4. Distribution of droplets on velocities. Tube of 5 mm diameter.

CONCLUSION

In conclusion, we note that the data obtained for the size and velocity distribution functions of droplets in the peripheral region of the gas--droplet flow make it possible to estimate the backflows of the droplet phase and to analyze the possibility of their reduction.

ACKNOWLEDGMENTS

This study was supported in part by the Russian Foundation for Basic Research (project No. 05-08-17981) and the International Science and Technology Center (project No. 2298p)

REFERENCES

1. V.N. Yarygin, V.G. Prikhodko, I.V. Yarygin, Yu.I. Gerasimov, A.N. Krylov, *Thermophysics and Aeromechanics*, Vol.10, №2, 269-286 (2003)
2. V.G. Prikhodko, G.A. Khramov, V.N. Yarygin, *Instruments and Experimental Techniques*, №2, 162-164 (1996)
3. V.G. Prikhodko, S.F. Chekmarev, V.N. Yarygin, I.V. Yarygin, *Doklady Physics (Doklady Academii Nauk)*, Vol.49, №2, 119-121 (2004)